ELSEVIER

Nuclear Instruments and Methods in Physics Research A 486 (2002) 214–219

NUCLEAR INSTRUMENTS & METHODS IN PHYSICS RESEARCH Section A

www.elsevier.com/locate/nima

Temperature dependence of the fast, near-band-edge scintillation from CuI, HgI_2, PbI_2, ZnO:Ga and CdS:In

Stephen E. Derenzo[a,*], Marvin J. Weber[a], Mattias K. Klintenberg[a,b]

[a] *Lawrence Berkeley National Laboratory, University of California, Mail Stop 55-121, 1 Cyclotron Road, Berkeley, CA 94720, USA*
[b] *Department of Physics, Uppsala Univeristy, Uppsala, Sweden*

Abstract

We present temperature-dependent pulsed X-ray data on the decay time spectra, wavelengths, and intensities of fast (ns) radiative recombination in five direct, wide-bandgap semiconductors: CuI, HgI_2, PbI_2, and n-doped ZnO:Ga and CdS:In. At 12 K the luminosity of powder samples is 0.30, 1.6, 0.40, 2.0, and 0.15, respectively, relative to that of BGO powder at room temperature. Increasing the temperature of CuI to 346 K decreases the luminosity by a factor of 300 while decreasing the fwhm of the decay time spectra from 0.20 to 0.11 ns. Increasing the temperature of HgI_2 to 102 K decreases the luminosity by a factor of 53 while decreasing the fwhm from 1.6 to 0.5 ns. Increasing the temperature of PbI_2 to 165 K decreases the luminosity by a factor of 27 while decreasing the fwhm from 0.52 to 0.15 ns. Increasing the temperature of ZnO:Ga to 365 K decreases the luminosity by a factor of 33 while decreasing the fwhm from 0.41 to 0.21 ns. Increasing the temperature of CdS:In to 295 K decreases the luminosity by a factor of 30 while decreasing the fwhm from 0.20 to 0.17 ns. All emission wavelengths are near the band edge. The luminosities decrease much faster than the radiative lifetimes, therefore, the reduction in luminosity is not primarily due to thermal quenching of the excited states, but mostly due to thermally activated trapping of charge carriers on nonradiative recombination centers. Since the radiative and nonradiative processes occur on different centers, increasing the ratio of radiative to nonradiative centers could result in a class of inorganic scintillators whose decay time and radiative efficiency would approach fundamental limits (i.e. <1 ns and 100 000 photons/MeV).

PACS: 78.60.H; 29.40.M; 29.40.W; 78.60; 72.20.J

Keywords: Wide band-gap semiconductors; Near-band-edge emission; Temperature-dependent scintillation

1. Introduction

Commonly used inorganic scintillators are, in many cases, either slow or have low radiative efficiency. For example, NaI:Tl, CsI:Tl, and $Bi_4Ge_3O_{12}$ are relatively efficient but have long decay times (>200 ns) because their transitions are spin forbidden. The core-valence luminescence of BaF_2 is fast but has a low radiative efficiency (<2000 photons/MeV) due to the low probability of forming holes in an upper core band. Currently, the inorganic scintillators with the best combination of speed and efficiency are Ce-doped, but their radiative decay times are limited to $\sim$10–60 ns due to the limited overlap of the 5d and 4f electronic orbitals. In this paper we explore five

*Corresponding author. Tel.: +1-510-486-4097; fax: +1-510-486-4768.

E-mail address: sederenzo@lbl.gov (S.E. Derenzo).

0168-9002/02/$ - see front matter
PII: S0168-9002(02)00705-2

direct wide-bandgap semiconductors, a neglected class of scintillators that provides the possibility of bright, sub-ns emission. The availability of such scintillators containing high proportions of atoms chosen for the efficient detection of particular ionizing radiation (e.g. X-rays, gamma-rays, neutrons) would substantially improve instrumentation for nuclear physics, high-energy physics, and medical imaging.

2. Fast, near-band-edge emission from direct gap semiconductors

Whereas compound semiconductors have been used extensively for conductivity radiation detectors (see, for example, Ref. [1]), several of these materials also have fast, near-band-edge emission that is potentially of interest for scintillation. In contrast with commonly used ionic scintillators, near-band-edge emitting semiconductors have excited states that extend over many atoms, and this involves negligible lattice relaxation. This emission may arise from band-to-band or free exciton recombination transitions. If the transition is direct and parity allowed, the radiative lifetime may be short, a nanosecond or less. Practical semiconducting crystals contain numerous defects and impurities that give rise to nonradiative recombination centers as well as free-to-bound, donor–acceptor pair, and bound exciton radiative transitions [2]. Consequently, the radiative efficiencies and decay times can vary from sample to sample.

An example of intentional doping to enhance fast, near-band-edge emission is the work of Lehmann on the direct semiconductors ZnO and CdS [3,4]. He showed in the mid-1960s that quenching could be reduced by n-doping these materials with Ga and In, respectively, and preparing them under reducing conditions. Scintillation from semiconductors has also been demonstrated by doping them with isovalent impurities. In the cases of CdS:Te [5] and ZnSe:Te [6], however, the lattice relaxation about the excited centers yields red-shifted emission and slower radiative decay rates.

3. Experimental measurements of luminosity and decay time

We have examined the temperature dependence of the fast, near-band-edge emission from three undoped and two doped semiconductors.

3.1. Materials

The CuI, PbI_2, and HgI_2 powders were purchased from Strem Chemicals with a metals purity $>99.999\%$. The ZnO:Ga(0.3%) and CdS:In(0.1%) powders were prepared by T. Perry of the Lawrence Livermore National Laboratory in collaboration with W. Lehmann. The powders were contained in fused silica cuvettes for measurements.

3.2. Pulsed X-ray system

This system, described more fully in Ref. [7], consists of an ultrafast laser system that delivers sub-ps pulses of 400 nm light onto the photocathode of a light-excited X-ray tube. Photoelectrons are accelerated to a tungsten anode at $+30$ kV to produce 35 ps (fwhm) pulses of X-rays with a mean energy of 18 keV [8]. Fluorescent photons from the sample are detected by a microchannel phototube with 35 ps (fwhm) response. The samples were cooled with an Advanced Research Systems, Inc. ARS2—A closed-cycle helium refrigerator.

Fig. 1 shows the overall system impulse response, determined by using a 1-mm thick PbF_2 crystal, painted black on five sides. In this material, recoil photoelectrons produce prompt bremsstrahlung radiation that is peaked at the low end of the photon energy spectrum. A small amount of fluorescence is also observed with a decay time of 28 ns and this component is not used in the impulse response.

3.3. Fitting procedures

To determine exponential decay times and fractions, the impulse response function was convolved with a sum of 30 components and their decay times and fractions were varied to minimize

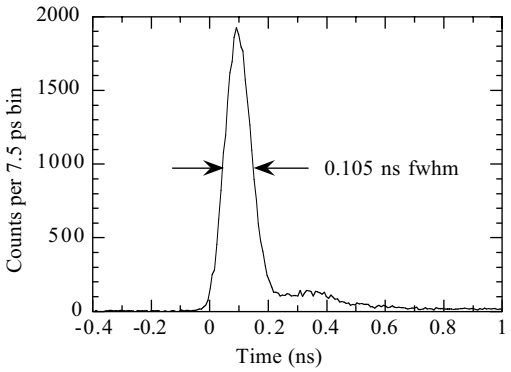

Fig. 1. Impulse response from a thin PbF_2 crystal painted black on five sides.

a log likelihood fit to the data [7]. Each of the decay times was constrained to lie within a narrow band and all fractions were constrained to be nonnegative.

4. Results

In the typical case of a sample with a luminosity comparable to that of room temperature BGO, two million events were recorded in 1 h. In each of the figures that follow, the decay time spectra are normalized to equal time measurements. In the tables to follow, the luminosities are reported only for components with decay times $<1\,\mu s$ and are normalized to BGO powder at 295 K in a fused silica cuvette (similar to those used for all the other samples). The luminosities and decay times/percentages are only accurate to about 20% of their value due to variability in sample placement and the well-known difficulty of fitting sums of exponentials to data.

4.1. Measurements of CuI

The emission spectrum of CuI (density 5.67 g/cm^3, bandgap 3.1 eV at 4 K) consists of weak, near-edge exciton bands and broad bands attributed to radiative recombination at lattice defects, the most intense of which occurs at $\sim$420–430 nm. There is a redistribution of intensities in the bands with increasing temperature, however, the free exciton band is observed up to 400 K [9].

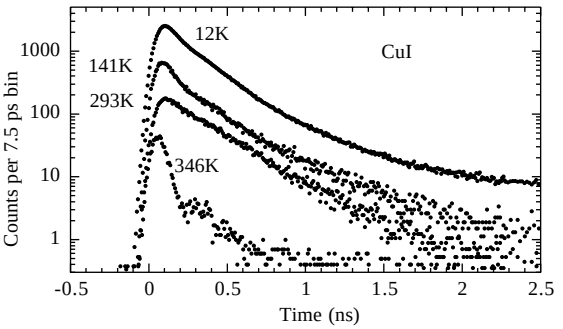

Fig. 2. Decay time spectra for CuI at four temperatures.

Table 1
Luminosity and principal fast decay times for CuI

Band edge	12 K	99 K	293 K	346 K
Luminosity	0.30	0.12	0.02	0.0013
fwhm (ns)	0.20	0.20	0.25	0.11
Component 1	0.12 ns	0.10 ns	0.13 ns	<0.05 ns
	58%	56%	28%	70%
Component 2	0.28 ns	0.29 ns	0.27 ns	0.13 ns
	26%	13%	62%	2%
Component 3	1.4 ns	1.1 ns	1.1 ns	0.7 ns
	7%	9%	5%	1%

Fig. 2 shows the decay time spectra for CuI at four temperatures; Table 1 lists the results of the fits to the data.

4.2. Measurements of HgI_2

The luminescence spectrum of tetragonal (red) mercuric iodide at 4 K (density 6.28 g/cm^3, bandgap 2.37 eV) consists principally of two bands: an exciton band at 2.33 eV and a featureless impurity/defect band at 2.22 eV. The latter band has been attributed to traps associated with iodine vacancies [10] and, more recently, to exciton annihilation at mercury vacancies [11]. Anderson has reported that the exciton–polariton decay rate decreases precipitously with increasing temperature [12]. The defect band luminescence exhibits a rapid rise time; the related formation rate is largely temperature independent and greater than the exciton

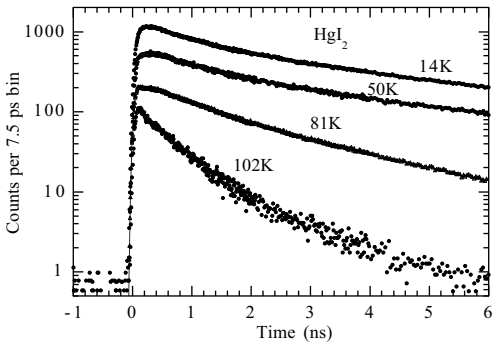

Fig. 3. Decay time spectra of HgI_2 at four temperatures.

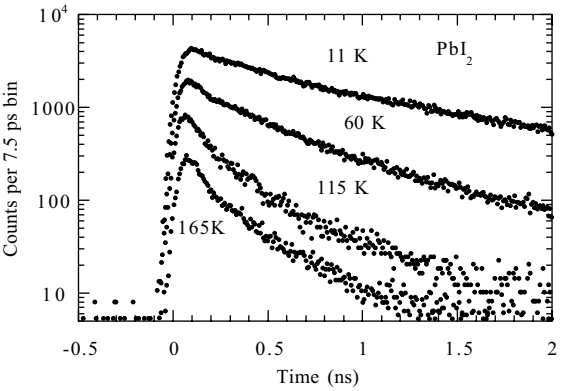

Fig. 4. Decay time spectra of PbI_2 at four temperatures.

Table 2
Luminosity and principal fast decay times for HgI_2

	14 K	50 K	81 K	102 K
Luminosity	1.6	0.80	0.18	0.03
fwhm	1.6 ns	1.5 ns	1.2 ns	0.5 ns
Component 1	0.6 ns	0.8 ns	0.75 ns	0.50 ns
	9%	10%	14%	48%
Component 2	2.0 ns	2.3 ns	1.7 ns	1.2 ns
	22%	22%	45%	34%
Slow components	> 5 ns	> 5 ns	> 5 ns	> 5 ns
	70%	68%	40%	17%

Table 3
Luminosity and principal fast decay times for PbI_2

Band edge	11 K	60 K	115 K	165 K
Luminosity	0.40	0.10	0.025	0.015
fwhm	0.52 ns	0.32 ns	0.16 ns	0.15 ns
Component 1	0.16 ns	0.16 ns	0.11 ns	0.06 ns
	10%	24%	50%	35%
Component 2	0.58 ns	0.43 ns	0.40 ns	0.29 ns
	25%	38%	24%	21%
Component 3	1.8 ns	1.3 ns	1.4 ns	1.4 ns
	43%	29%	10%	11%

decay rate. With increasing temperature the decay rates of the two bands become comparable. Nonradiative decay dominates at temperatures > 100 K. Scintillation in HgI_2 has been reported briefly [13].

Fig. 3 shows the decay time spectra for HgI_2 at four temperatures; Table 2 lists the results of the fits to the data.

4.3. Measurements of PbI_2

Th emission spectrum of PbI_2 at low temperatures (density 6.16 g/cm^3, bandgap 2.55 eV) consists of near-edge lines due to free and bound excitons and broad overlapping bands shifted by ~100–200 meV attributed to donor–acceptor pair transitions [14–16].

Fig. 4 shows the decay time spectra for PbI_2 at four temperatures; Table 3 lists the results of the fits to the data.

4.4. Measurements of ZnO:Ga

The introduction of ~0.3% Ga into ZnO (density 5.61 g/cm^3, bandgap 3.44 eV at 4 K) introduces a degenerate donor band overlapping the bottom of the conduction band and increases the conductivity of the material. The edge emission spectrum at low temperatures reflects the density of states; at room temperature it is a broad band extending from ~3.1 to 3.3 eV [4].

Fig. 5 shows the decay time spectra for ZnO:Ga at four temperatures; Table 4 lists the results of the fits to the data.

4.5. Measurements of CdS:In

At high doping levels, the conduction band of CdS:In (density 4.83 g/cm^3, bandgap 2.58 eV) is degenerate and partly filled with donor electrons.

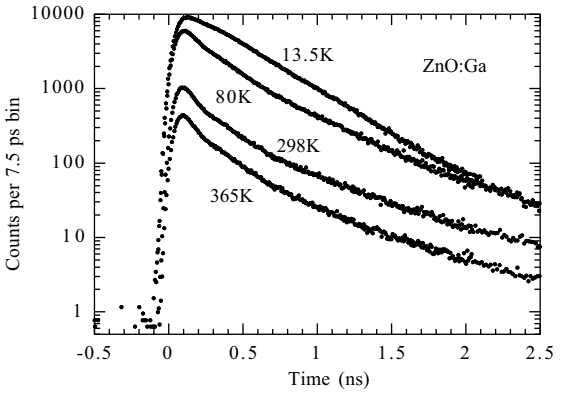

Fig. 5. Decay time spectra of ZnO:Ga at four temperatures.

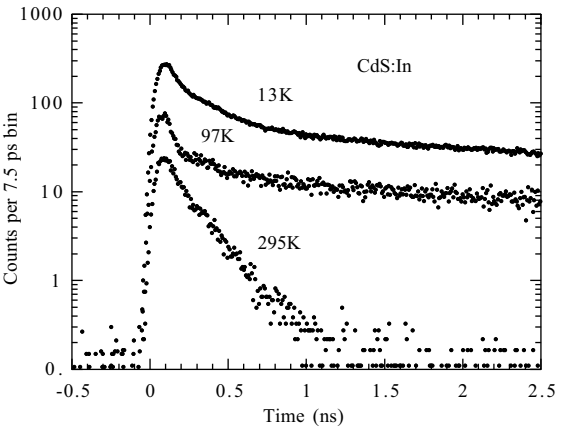

Fig. 6. Decay time spectra of CdS:In at three temperatures.

Table 4
Luminosity and principal fast decay times for ZnO:Ga

	13.5 K	80 K	295 K	365 K
Luminosity	2.0	1.0	0.15	0.06
fwhm (ns)	0.41	0.27	0.21	0.21 ns
Component 1		0.14 ns	0.11 ns	0.11 ns
		45%	39%	37%
Component 2	0.30 ns	0.35 ns	0.32 ns	0.29 ns
	80%	17%	23%	23%
Component 3	0.54 ns	0.60 ns	0.82 ns	0.78 ns
	18%	32%	30%	28%

Table 5
Luminosity and principal fast decay times for CdS:In

	13 K	97 K	295 K
Luminosity	0.13	0.035	0.001
fwhm (ns)	0.20	0.14	0.17
Component 1	0.10 ns	0.31 ns	0.12 ns
	13%	8%	95%
Component 2	1.2 ns	0.73 ns	2.2 ns
	11%	7%	4%
Component 3	7 ns	6 ns	
	43%	43%	
Component 4	21 ns	21 ns	
	32%	43%	

Emission is due to non-k-conserving band-to-band transitions [17,18]. The width and peak wavelength of the band change with changing In concentration [4]. At 0.1% In the edge emission spectrum at room temperature is a featureless band that extends from $\sim$2.2 to 2.5 eV.

Fig. 6 shows the decay time spectra for CdS:In at three temperatures; Table 5 lists the results of the fits to the data.

5. Discussion

Because we are interested in the total luminosity change with temperature, no spectral filtering was used in obtaining the above results. Thus the observed scintillation at low temperatures may involve free and bound exciton emission, free-to-bound carrier emission, and donor–acceptor pair transitions. The nonexponential decay of the iodides at low temperature is suggestive of donor–acceptor recombination emission.

A characteristic immediately evident in the above results is that at all but the highest temperatures, increasing the temperature results in large changes in sample luminosity but only small changes in decay time(s). This is in contrast to normal thermal quenching where increasing the temperature decreases both the luminosity and decay time at the same rate. From this we conclude that (1) the number of radiative excited states is controlled by the temperature and the activation energy for competitive trapping of charge carriers on nonradiative centers, and (2) the radiative

excited states, once formed, are not subject to quenching. The luminosity vs. temperature data reveal the existence of one or more activation energies for nonradiative trapping in the range of tens to hundreds of meV.

At the highest temperatures the decay time begins to decrease. A similar luminosity and decay time behavior also has been reported for GaN, and attributed to thermal detrapping of holes from acceptor atoms [19,20].

The observed luminosities at low temperatures are comparable to that of BGO at 295 K (8200 photons/MeV) and thus are much less than expected if there were no initial nonradiative recombination or trapping of charge carriers. Nevertheless, the present materials are potentially useful scintillators at low temperatures. To improve efficiency and make possible higher temperature operation, one needs to reduce the number of nonradiative recombination centers and/or introduce acceptor levels such that the probability of radiative transitions to these levels is more competitive with nonradiative recombination rates. This would result in fast, bright scintillation.

Acknowledgements

We thank W. Moses, E. Haller, and R. Williams for helpful discussions, Sang Oh and M. Ho for technical assistance, and T. Perry for samples of ZnO:Ga and CdS:In. This work was supported in part by the Director, Office of Science, Office of Biological and Environmental Research, Medical Science Division of the US Department of Energy under Contract no. DE-AC03-76SF00098 and in part by Public Health Service Grant no. R01 CA48002 awarded by the National Cancer Institute, US Department of Health and Human Services. M.K. acknowledges Stiftelsen för Internationalisering av Högre Utbildning och Forskning (STINT), The Royal Swedish Academy of Science (KVA) and Göran Gustafsson Stiftelse for financial support. Reference to a company or product name does not imply approval or recommendation by the University of California or the US Department of Energy to the exclusion of others that may be suitable.

References

[1] D.S. McGregor, H. Hermon, Nucl. Instr. and Meth. A 395 (1997) 101.
[2] P.Y. Yu, M. Cardona, Fundamentals of Semiconductors, 3rd Edition, Springer, Berlin, 2001, pp. 345–369.
[3] W. Lehmann, J. Electrochem. Soc. 112 (1965) 1150.
[4] W. Lehmann, Solid-State Electron. 9 (1966) 1107.
[5] P. Schotanus, P. Dorenbos, V.D. Ryzhikov, IEEE Trans. Nucl. Sci. NS-39 (1992) 546.
[6] V. Ryzhikov, N. Starzhinsky, L. Gal'chinetskii, et al., IEEE Trans. Nucl. Sci. NS-48 (2001) 356.
[7] S.E. Derenzo, M.J. Weber, W.W. Moses, et al., IEEE Trans. Nucl. Sci. NS-47 (2000) 860.
[8] S.C. Blankespoor, S.E. Derenzo, W.W. Moses, et al., IEEE Trans. Nucl. Sci. NS-41 (1994) 698.
[9] V.A. Nikitenov, V.I. Popolitov, S.G. Stoyukhin, et al., Sov. Tech. Phys. Lett. 5 (1979) 493.
[10] J.L. Merz, Z.L. Wu, L. van den Berg, et al., Nucl. Instr. and Meth. 213 (1983) 51.
[11] I.Kh. Akopyan, B.V. Bondarenko, O.N. Volkova, et al., Phys. Solid State 39 (1997) 58.
[12] R.J.M. Anderson, Nucl. Instr. and Meth. A 380 (1996) 88.
[13] B.V. Shulgin, S.I. Gorkunova, V.L. Petrov, et al., in: P. Dorenbos, C.W.E. van Eijk (Eds.), Proceedings of the International Conference on Inorganic Scintillators and their Applications, SCINT'95, Delft University Press, The Netherlands, 1996, pp. 459–461, pp. 469–471.
[14] R. Kleim, F. Raga, J. Phys. Chem. Solids 30 (1969) 2213.
[15] S. Yamazaki, T. Goto, J. Phys. Soc. Japan 51 (1982) 3228.
[16] V.A. Bibik, N.A. Davydova, Phys. Status Solidi A 126 (1991) K191.
[17] Ch. Frick, U. Neukirch, R. Heitz, et al., J. Crystal Growth 117 (1992) 783.
[18] U. Neukirch, I. Broser, R. Rass, Phys. Status Solidi B 159 (1990) 431.
[19] M. Leroux, N. Grandjean, B. Beaumont, et al., J. Appl. Phys. 86 (1999) 3721.
[20] M. Smith, G.D. Chen, J.Y. Lin, et al., Appl Phys. Lett. 68 (1996) 1883.